

Seasonal characterization of tropospheric ozone fluctuation in Mexico City

S. Matias-Gutierrez

*Department of Environmental Engineering, Instituto Tecnológico de Estudios Superiores del Oriente del Estado de México, State of México, México. Applied Research In Earth Science.
e-mail: smatias@ipn.mx*

E. I. García-Otamendi

*Department of Information Technologies, Universidad Autónoma del Estado de Hidalgo, ESTi Campus.
e-mail: edgar_garcia@uaeh.edu.mx*

L. Morales-Ruíz

*Applied Research In Earth Science,
e-mail: leomorr@yahoo.com*

L. Palacios-Luengas

*Department of Electrical Engineering, Universidad Autónoma Metropolitana, Iztapala Campus.
e-mail: lpluengas@protonmail.com*

Received 23 June 2022; accepted 28 August 2022

The air pollution due to tropospheric ozone (O_3) is one of the most serious problems of large industrialized cities in the world. The excessive increase in O_3 has a negative impact on the population health. Consequently, researchers have focused their efforts establishing measures to characterize the statistical analysis of spatio-temporal data. This work shows a study based on seasonal analysis of spatio-temporal data through second order structure function to and the scale behavior in power law by using the Hurst exponent (H) and analyzing the trend of fluctuations associated with O_3 pollution concentration records at four monitoring stations in the Metropolitan Area of Mexico City (MAMC) considering the four season of the year. The records were consulted from the database of the Automatic Atmospheric Monitoring Network (AAMN) in Mexico City from 2010 to 2018. The results show the differences in behavior of ozone according to the seasons of the year in this megacity. The behavior of statistical persistence predominates in spring, with 63.89% of occurrence over the total of the samples analyzed. In winter, the observed regime is antipersistent, with 80.56%. The three regimes: persistence, randomness and antipersistence were observed in summer and autumn, with a similar proportion of occurrence of $33\% \pm 3\%$. Given the above, the climatological characteristics of each season could be associated with the regimes of persistent, random and antipersistent behavior of the fluctuation of the concentration of the pollutant O_3 .

Keywords: Structure function; ozone (O_3); air pollution in Mexico City; Hurst exponent; monitoring stations; persistence.

DOI: <https://doi.org/10.31349/RevMexFis.69.021402>

1. Introduction

Tropospheric ozone (O_3) is formed from the chemical reaction between the action of sunlight and different precursor substances such as volatile organic compounds, carbon monoxide (CO) and nitrogen oxides, among others studied by [1]; it has origin in combustion processes from industrial emissions and vehicular traffic defined by [2]. Given the nature of O_3 in large cities, it is subject of numerous studies that show its adverse effects on health [3-5]. For this reason, studies of the temporal records of O_3 have been carried out to understand its behavior from data analysis [6,7]. Also, it have been found the climatic variables play an important role in the process of accumulation or dispersion of O_3 concentration levels [8,9]. For example, in the Klang Valley, Malaysia between January 1997 and December 2006, the analysis show that the concentrations of some pollutants, such as CO , NO_2

and SO_2 , are higher in the stations that report the heaviest traffic and the concentrations of PM_{10} and O_3 are influenced by regional tropical factors, biomass burning, and ultraviolet radiation [10]; furthermore, they considered significant differences between pollutant concentrations in different monitoring stations, suggesting that the local environment influences the concentration of gases in each season. In similar way, in Malaysia during period from 1999 to 2010, it were reported in their study variations in O_3 levels due to meteorological variables with highest concentrations in the first quarter of 2009 [11]. Also, they show that the average O_3 concentration was higher in February and lower in November.

The evaluation of O_3 contaminants carried out by [12], in Deradun, India, consider environmental volatile organic compounds (VOC) samples for three seasons: summer, winter and the monsoon. They report that recorded toluene en-

environmental concentration is higher during winters and lower in monsoons. According to [12], the high toluene proportion indicates vehicular emission as the main source, because toluene and xylenes are found in the hydrocarbons that contribute the most to O_3 formation [13], in the city of Tenerife, describe the influence of climatic conditions and find that the PM_{10} are lower during the rain and describe the temporal evolution of the pollutant concentrations, O_3 included.

On the other hand, the findings in the literature suggest several underlying relationships between meteorology, anthropogenic sources, and pollutant concentrations that are useful for establishing local trends in air pollution over time and geographical space. Hence, a large number of researchers have focused their efforts on characterizing O_3 contamination records among others [14-17]. To accomplish this, they make use of Fractal theory tools due to the complex and chaotic nature of the phenomenon. Consequently, it has been possible to characterize data series of different environmental pollutants with a small data set.

This paper is structured as follows. In Sec. 2, state of the art review on statistical persistence studies of air pollutant records in different cities in the world are considered. Section 3 describes the performed analysis using seasonal fluctuation and structure function to that characterize long-term correlations of the data series. Section 4 shows the results obtained to explain the behavior of the data series for the different seasons of the year in Mexico City. Finally, in Sec. 5, conclusions are described.

2. State of the art review

In the last decades, studies have been conducted on the statistical persistence in air pollutant records in different cities around the world [18-23]. It was also established that time series associated with different air pollutants are complex systems and multifractal in nature [24-28]. The multifractal behavior was characterized under different analysis metrics, from those referred to as FA fluctuation analysis, FDA detrended fluctuation analysis, rescaled range, spectral analysis, two-dimensional multifractal detrended fluctuation analysis (2D-MFDMA) [18,26,27,29]. A study on air quality index (AQI) time series for CO , NO_2 , O_3 , $PM_{2.5}$, PM_{10} and SO_2 pollutants using multifractal fluctuation detrended analysis (MF-FDA) was carried out by [28]; He found multifractal behaviors for pollutant concentration series for Beijing, Jinan and Zhengzhou cities in China. In other study conducted on API time series between 2001 and 2012 in Nanjing, China, the multifractal nature and long-term correlations were reported by [25]. Furthermore, the existence of multifractal nature and statistical persistence, *i.e.*, long-range correlations, for major air pollutants O_3 , SO_2 , CO , NO_2 , and PM_{10} , in Mexico City, have also been empirically demonstrated, as can be seen in Refs. [20,24]. On the other hand, analysis on atmospheric pollutants from a classical fractal model and the fluctuation associated with these series of records were conducted on other works. For example, during the period

1993-1999, studies of pollutants O_3 , PM_{10} and PM_2 , using Sigma-T (ST), Hurst and the rescaled range to determine the Hurst exponent index were carried out in the United Kingdom by [30]. They found persistence of pollutant fluctuation over a temporal period of days. Detrended fluctuation analysis (DFA) on time series of O_3 , NO_x and PM_{10} , for the cities of Athens, Greece and Baltimore, USA, were performed by C.A. Varotos, *et al.*, [30]. They found that while O_3 and NO_x pollutants show persistence in time scales ranging from one week to five years; for PM_{10} persistence appears at intervals of four hours to nine months. Also, the Detrended Moving-Median (DMM) method to estimate both the Hurst persistence degree and persistence properties of ozone concentrations, from eight air quality monitoring stations in urban and suburban areas of peninsular Malaysia, was used by [32]. The previous studies empirically determine the multifractal condition of the time series of atmospheric pollutants in different cities of the world, including Mexico City; as well as the persistence associated with the time scale. In addition to this, other works report the influence of both meteorological factors, *i.e.*, temperature, humidity and wind speed [26]; and seasonal effects, on concentration levels through long-term correlations [18]. However, as it is well known, quantitatively the formation, deposition and distribution of pollutants in the environment are characteristic of the dynamics of environmental factors and anthropogenic activities in each region of the world [33-35]. Then, it is important to understand the extrinsic information of the factors influencing the time series behavior of various atmospheric pollutants with respect to seasonal dynamics. For this reason, a local analysis is proposed to examine the statistical persistence associated with the time scale of the influence of meteorological factors implicitly associated with the dynamics of each season of the year.

In this work we use a metric that determines the characteristic behavior of time series (in the context of the Hurst exponent), in particular those associated with O_3 records from four different RAMA sites in Mexico City. Consequently, a quantitative estimation of the statistical behaviors of persistence, antipersistence and randomness of the spring, summer, autumn and winter seasons of each year analyzed is given.

3. Methodology

We analyze the fluctuations of the time series associated with O_3 in Mexico City during 2010-2018, and determining the persistence in the seasonal periods, *i.e.*, Spring, Summer, Autumn, and Winter, through the dynamic scaling approach using the structure function [36]. In this work, the used records of O_3 concentration indices were obtained from Automatic Atmospheric Monitoring Network (AAMN) of Mexico City from four different monitoring stations: Cuajimalpa (CUA), Merced (MER), Tlalnepantla (TLA), and Xalostoc (XAL), according to Fig. 1. The concentration indices correspond to a nine-year period, from 2010 to 2018, and time series are

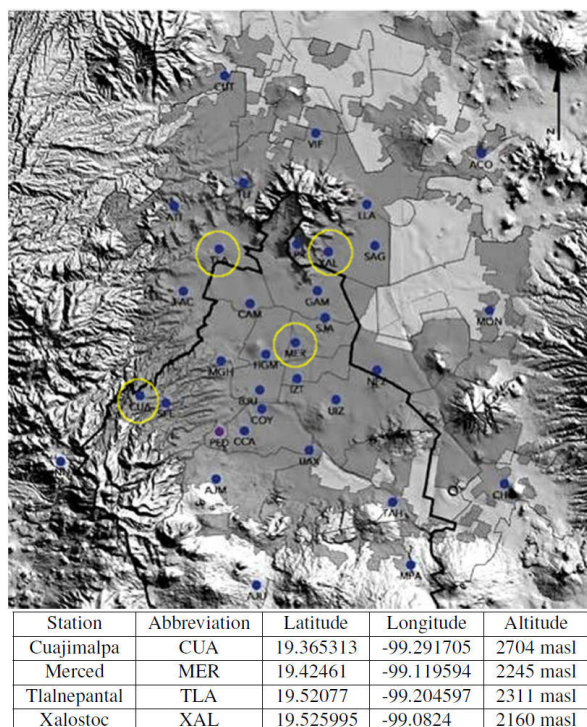


FIGURE 1. Location of air quality monitoring stations in Mexico City.

constructed from data of the seasonal periods Spring, Summer, Autumn, and Winter. The persistence of these seasonal periods is studied by determining the Hurst exponent (H) for the fluctuation associated with these time series by means of the second order structure function.

3.1. Data collection

The Atmospheric Monitoring System (AMS) of Mexico City is responsible for the permanent measurement of the main air pollutants (SO_2 , NO_2 , CO , O_3 , PM_{10} , and $\text{PM}_{2.5}$), AAMN is made up of 29 monitoring stations and provides immediate information for activation or deactivation of alert or emergency procedures for environmental contingency. In addition, it has historical records of the pollutants of Mexico City and the metropolitan area (<http://www.aire.cdmx.gob.mx/default.php>). Hence, the daily records by hour of O_3 from January 1, 2010 to December 31, 2018 of the CUA, MER, TLA, and XAL monitoring stations are considered. Figure 2 shows the total records from each site with their respective concentration variation in parts per billion (ppb).

The following data for each monitoring station are considered: 56217 records were taken from CUA, 56239 records from MER, 54744 records were 140 taken from TLA and 58687 records from XAL. In general, there are 9 years of records corresponding to four monitoring sites, for a total of 36 samples for each season of the year (see Table I). Notice the data differences of the consulted records, this is because in some hours the monitoring station were in maintenance or

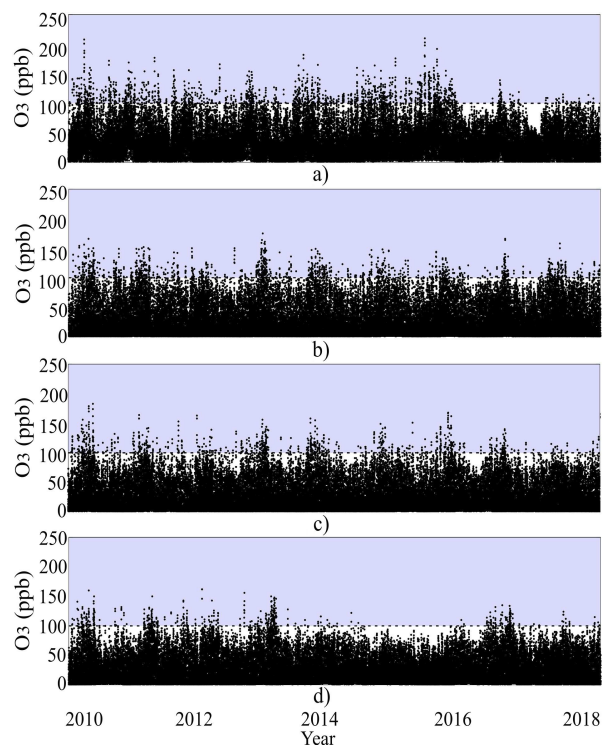


FIGURE 2. O_3 concentration profiles of four monitoring stations: a) CUA, b) MER, c) TLA and d) XAL.

calibration (See Table I). Each site was chosen because they manifest highest levels of O_3 in Mexico City. For example, XAL corresponds to an area composed of a high vehicular traffic that connects the Metropolitan area in the northern part of Mexico City, and every day around 1.5 million people mobilize to carry out their work and education activities. In addition, it has an industrial zone, that is considered one of the most polluted areas in Mexico. TLA is another area that is immersed in the Valley of Mexico and it is part of the most polluted places in the country providing 18% of greenhouse gases. MER is in the center of Mexico City with commercial and vehicular traffic activities. CUA is in the southwest of Mexico City and it is considered one of most O_3 polluted places 80% of its surface correspond to ecological protected areas.

3.2. Seasonal fluctuation

The methodology used in this work is based on the fluctuation analysis (FA), it since allows the detection of long-term correlations in time series. From a time series $\{x(t) : t = 1, 2, \dots, N\}$ with a nonzero mean, a new time series is constructed $y(t)$, which is determined by the cumulative sum of $x(t)$ [37], and the fluctuation function $Y(t)$ is obtained as shown in Eq. (1) and Fig. 5.

$$Y(t) = y(t) - \hat{y}(t), \quad (1)$$

where $\hat{y}(t)$ is a first-degree polynomial function, and is the tendency associated with the function $y(t)$ [38].

TABLE I. Total data analyzed by monitoring station by year and season.

Monitoring Station	Year	Spring	Summer	Autumn	Winter	Total data
CUA	2010	2188	1674	1859	53	56217
	2011	1564	1760	1584	263	
	2012	2210	2226	2082	256	
	2013	2141	2116	1827	249	
	2014	2083	1605	1934	259	
	2015	2214	2180	2160	258	
	2016	2197	1965	2108	254	
	2017	2118	1828	2102	256	
	2018	2156	2168	2062	258	
MER	2010	2052	1900	1787	64	56239
	2011	2053	1956	2038	244	
	2012	2097	2093	2076	256	
	2013	2058	2065	1962	207	
	2014	2081	1939	1798	259	
	2015	2187	2077	2072	254	
	2016	1896	2073	1776	257	
	2017	2143	1922	1866	256	
	2018	2128	2110	2012	225	
TLA	2010	1910	1776	1821	228	54744
	2011	2111	2033	1999	248	
	2012	1889	1892	1738	251	
	2013	2059	2013	1641	251	
	2014	2008	2076	1902	259	
	2015	2175	2177	1916	258	
	2016	2019	1593	2110	226	
	2017	2173	2179	1873	254	
	2018	1803	1609	2016	258	
XAL	2010	2182	2161	2184	263	58687
	2011	2141	2186	2160	243	
	2012	2146	2099	2184	257	
	2013	1885	2166	2184	258	
	2014	1850	2188	2184	166	
	2015	2208	2168	2160	258	
	2016	1389	2099	2184	257	
	2017	2191	2138	2184	252	
	2018	1869	1800	2184	259	

$X_m(t_n)$ is obtained from $x(t)$ for each season, where $m =$ Spring, Summer, Autumn and Winter, $t_n \in [1, N]$ and $n = 1, 2, 3, 4, \dots$. Note that Fig. 3 shows the variation of O_3 concentration profiles for each season of the year 2010 for CUA monitoring station, defined by $x_m(t_n)$. It is also noted that the number of records varies according to the season and time of year considered. Using Eq. (1) in $X_m(t_n)$ gives the fluctuation function $Z_m(t_n) = y_m(t_n) - \hat{y}(t_n)$ where the cu-

mulative sum is $y_m(t_n) = \sum X_m(t_n)$. The hourly mean of the O_3 concentration variations can be seen in Fig. 4.

3.3. Structure function

The Structure function used in turbulence analysis establishes the scale dependence in power law of the fluctuation function. In addition, it exhibits correlation of time sequences [36,39].

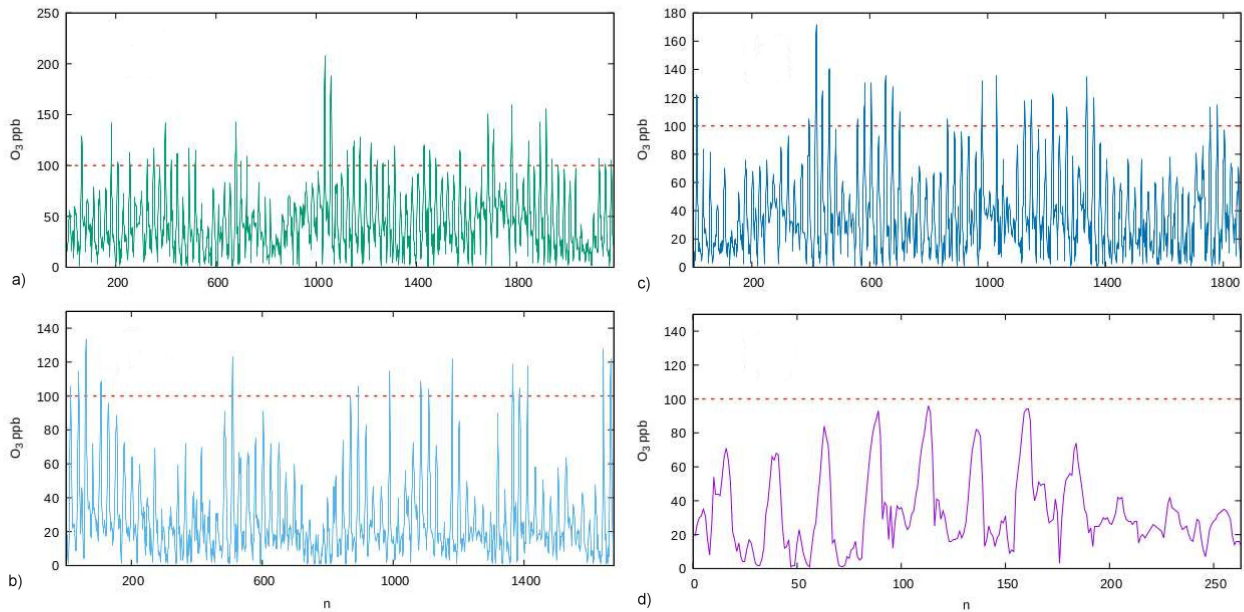


FIGURE 3. O₃ concentration variation of seasonal sites for CUA monitoring station in 2010: a) Spring, b) Summer, c) Autumn and d) Winter.

To characterize the behavior of the fluctuation series $Z_m(t_n)$, the use of the Structure function $F_2(\Delta_n)$ is proposed. The second order Structure function is defined by Eq. (2) [40].

$$F_2(\Delta_n) = \sqrt{\frac{1}{N - \Delta_n} \sum_{n=1}^{N - \Delta_n} |Z_m(t_n) - Z_m(t_n + \Delta_n)|^2}. \quad (2)$$

The window width or sampled interval $\Delta_n \in [1, N]$ with a data series length N . Thus, considering that for time series with long-range correlations, $F_2(\Delta_n)$ is expected to exhibit a behavior in power law $F_2(\Delta_n) \propto (\Delta_n)^H$ with $H \in [0, 1]$ and H is identified as Hurst exponent [41,43]. Then, H characterizes the invariance of statistical scale associated with long and short-range correlations. For this, the following criterion is considered: short-term negative correlation if $0 < H < 0.5$ indicates antipersistence, $H = 0.5$ indicates randomness, and if $0.5 < H < 1$ indicates persistence, that is, it shows correlations of long range [44].

4. Analysis and discussion of results

4.1. Descriptive analysis

According to Fig. 2, the O₃ variation in four different monitoring stations (CUA, MER, TLA, and XAL) from January 1, 2010 to December 31, 2018, indicate the maximum levels allowed by the World Health Organization [45] and the Official Mexican Standard NOM-020-SSA1-2014 [46] for air quality. Note that the values above the dotted line indicate afflictions mainly in the airways and consequently the health of people. However, the O₃ concentration records that exceed the permissible threshold of 100 ppb have few incidents. The high occurrences index of maximum permissible O₃ observed throughout the study period suggests conducting studies in a contamination range of O₃ > 100 ppb to neglect the

existence of trends and was possibly due to situations that were atypical (see Table II).

Meraz *et al.*, observed a decrease in O₃ concentration in the nineties and non-decreasing seasonality for 2007, therefore it is stated that the dynamics of O₃ have changed dramatically in this studied decade [20].

Figure 4 shows the O₃ record values for the different monitoring sites corresponding to: a) MER, b) XAL, c) TLA and d) CUA, for the analysis period 2010-2018. For each hour of the day, the values of O₃ records were averaged considering the data corresponding to each of the seasons of the year (spring, summer, autumn and winter), but not only for a single year, but for the entire period 2010-2018. It is observed that the maximum O₃ records occur in the range from 14

TABLE II. Number of occasions that concentration values were over 100 ppb, total in each station for the 2010-2018 period and total per season.

Monitoring station	Spring	Summer	Autumn	Winter	2010-2018
MER	717	123	107	25	972
XAL	332	18	70	3	423
TLA	480	71	96	6	653
CUA	734	346	229	11	1320
Total	2263	558	502	45	3368

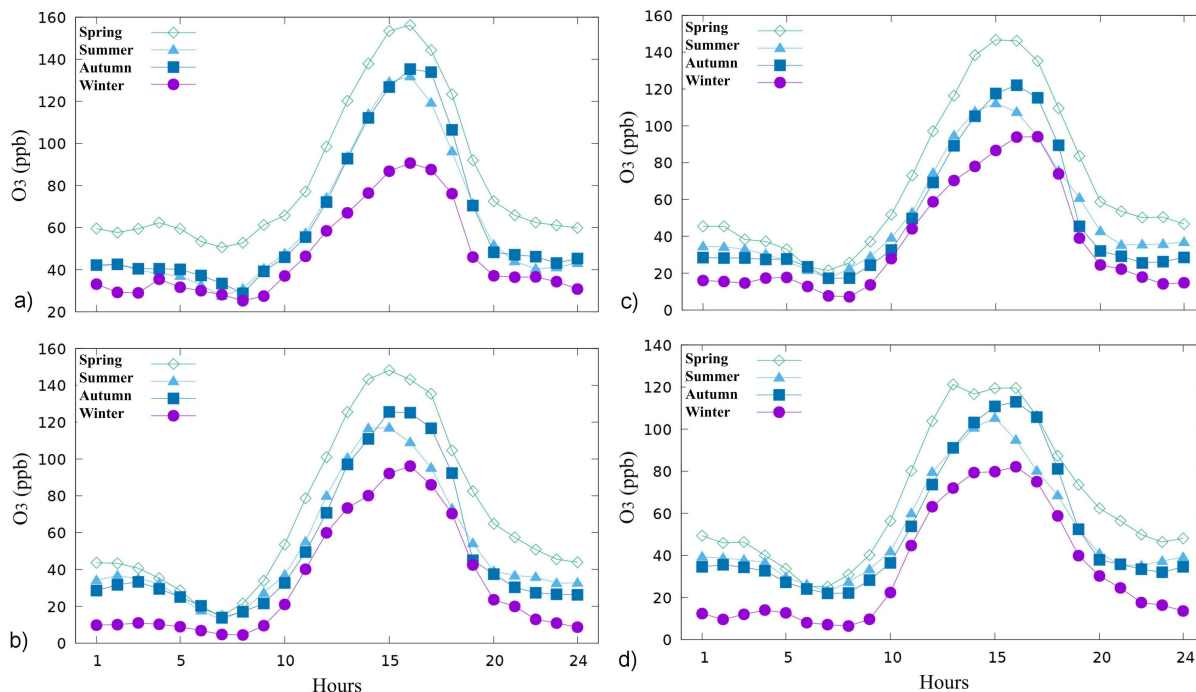


FIGURE 4. O₃ concentration variations hourly mean in the 2010-2018 period for: a) MER, b) XAL, c) TLA and d) CUA.

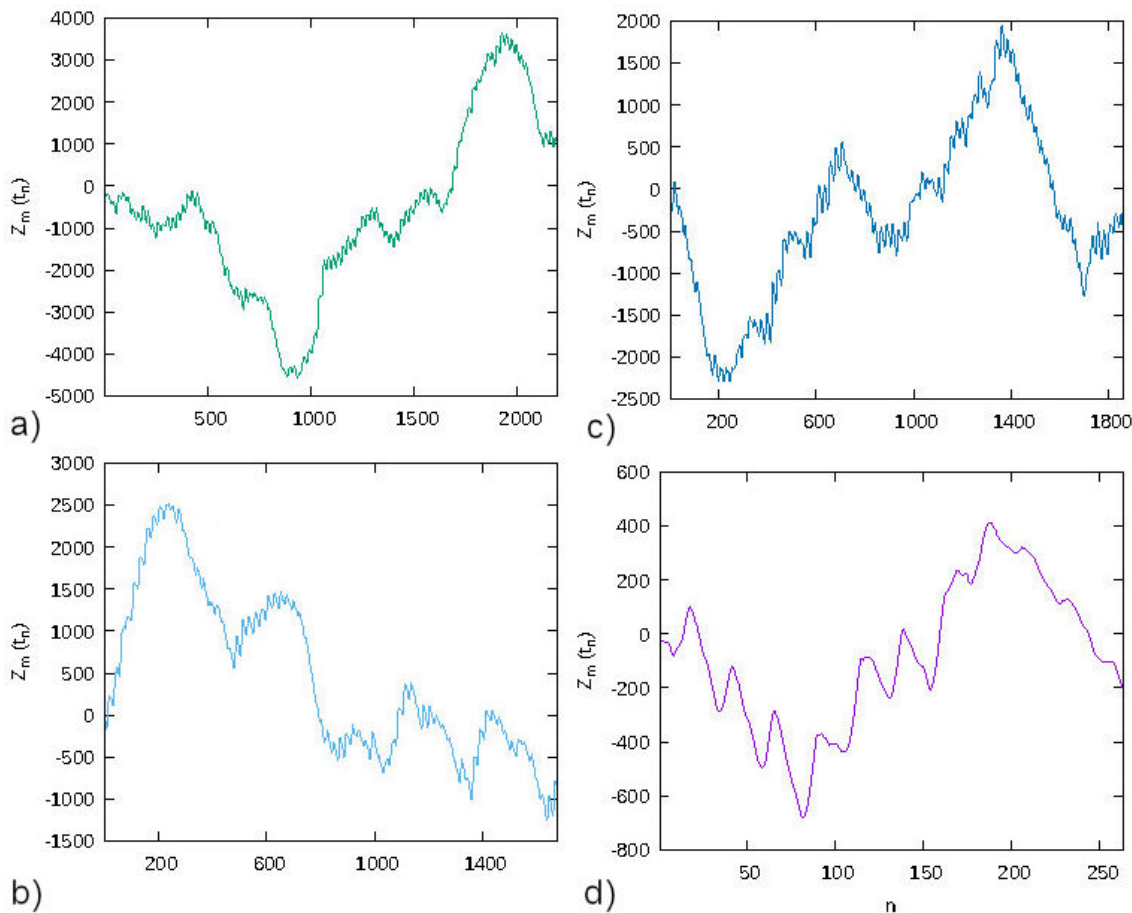


FIGURE 5. Fluctuation function associated with the O₃ concentration variations corresponding to the year 2010 for: a) Spring, b) Summer, c) Autumn and d) Winter.

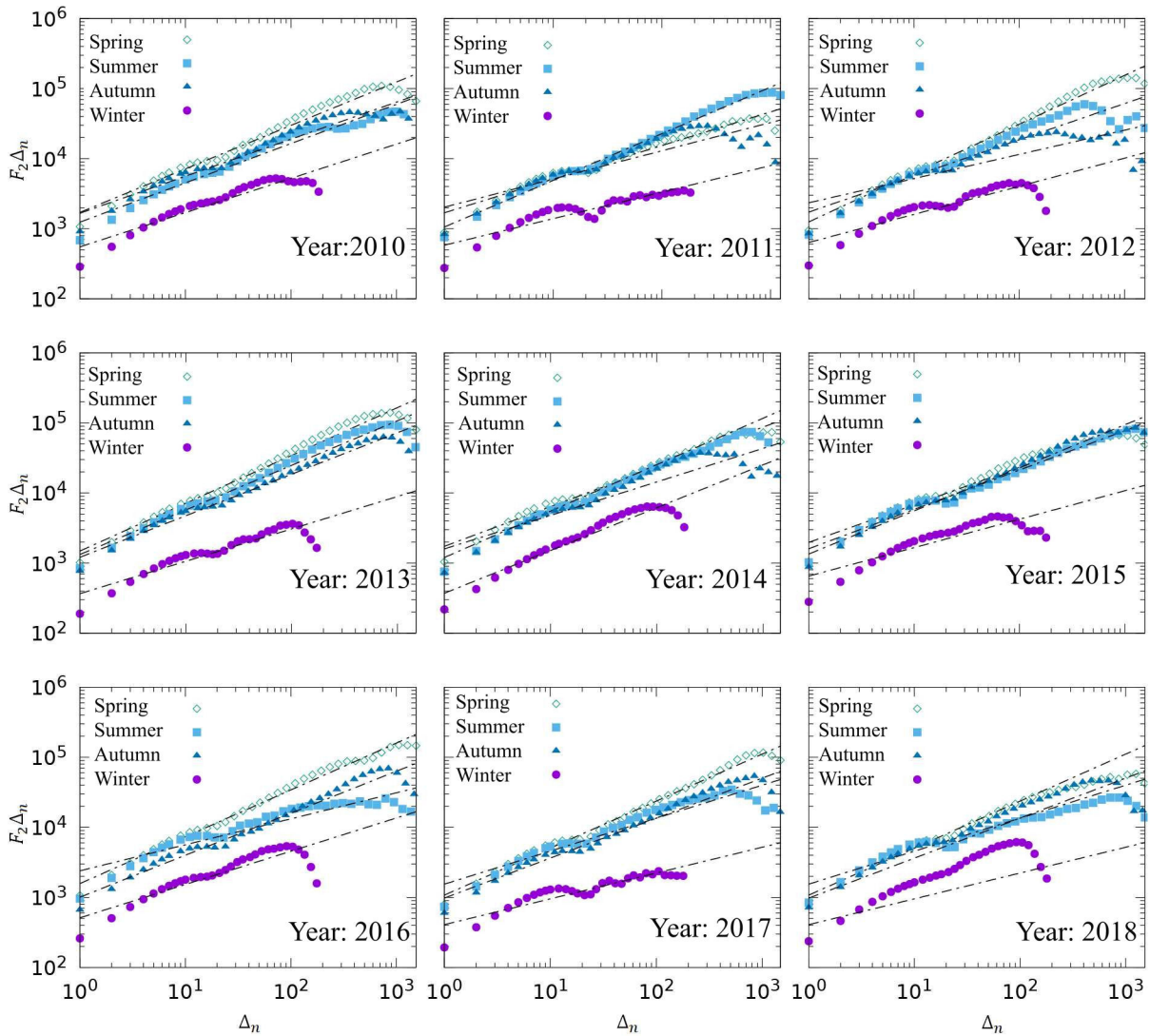


FIGURE 6. Structure function $F_2(\Delta_n)$ for different Δ_n sizes for: Spring, Summer, Autumn and Winter from to CUA monitoring station.

to 17 hrs with values ranging from 80 ppb to 160 ppb for the four sites and stations studied; analogous observations can be seen in Refs. [47-50]. We also note in this Fig. 4 that the magnitudes of the spring maximum O_3 records are always higher than the magnitudes of the winter maximum O_3 records. A similar behavior in O_3 concentration variations is maintained in different monitoring sites in Seul Corea for the four seasons of the year as observed by [51]. For the summer and fall at the four monitoring sites studied, the magnitude of the maximum records is lower than those observed in spring, but higher than those observed in winter. Locally, monitoring sites show differences regard O_3 concentration levels. Higher values are found for MER, XAL, and TLA sites, while the lowest concentration values are observed for CUA.

In addition, the maximum record values of the pollutant O_3 , which exceed the limits allowed by the Mexican official standard NOM-020-SSA1-2021 and have led to environmental contingencies, are observed too in the spring, summer and winter seasons. Figure 5 shows the fluctuation function con-

structed from O_3 concentration profiles (Fig. 3) concentration variations of CUA for Spring, Summer, Autumn and Winter during 2010.

For the Structure function considering Spring, Summer, Autumn and Winter seasons corresponding to CUA, scaling in power law are consider to exist, according to the log-log graph of Fig. 6. It can be seen that the slope corresponds to H sampled from the four monitoring stations during the 2010-2018 period. An average value of H is estimated during the indicated period of the four monitoring zones for the Spring, Summer, Autumn and Winter seasons.

4.2. Structure function analysis

Figure 6 shows the scaling in power law of the fluctuations associated with O_3 concentration variation of the CUA monitoring station for the 2010-2018 period. Note that for Spring, Summer and Autumn seasons, it is observed a scale up to three orders of magnitude, where H is determined by the re-

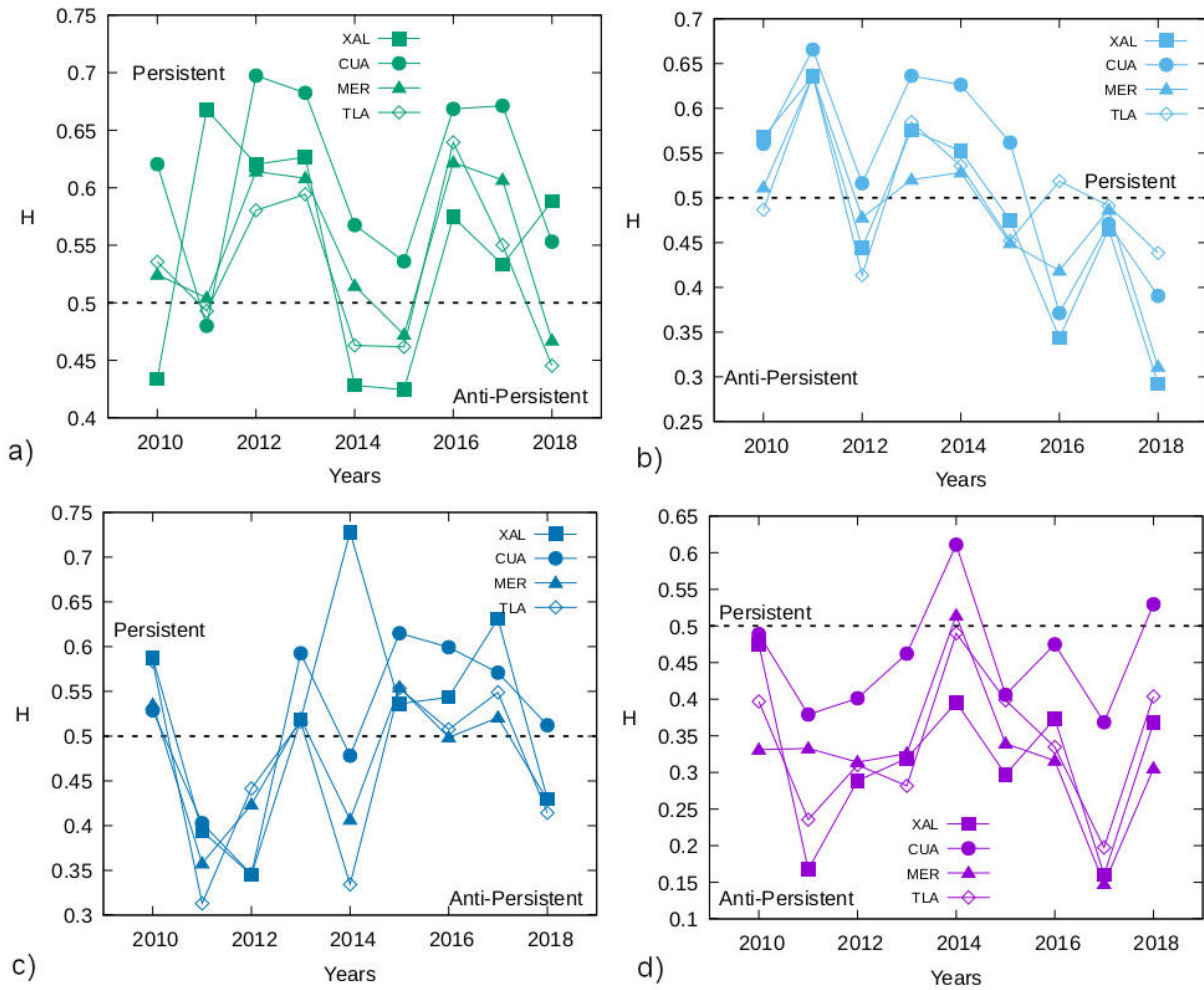


FIGURE 7. Hurst exponent distribution for year: a) Spring, b) Summer, c) Autumn and d) Winter.

lation $\log F_2(\Delta n) \sim \log(\Delta n)^H$. Table III, and Fig. 7 show the influence of temporality in the four monitoring stations. According, it is observed that the Spring season of the CUA, XAL, TLA, and MER monitoring stations predominates the trend of H to statistical persistence, with an occurrence rate of 63.8% and $\bar{H} = 0.61$, which implies that the O_3 concentration variation values subsequently registered and in process maintain the sign of the variations [32].

If the registered O_3 levels reach relatively high values, then the system tends to keep them high, indicating that it is limited by the scaling range where the power law predominates, and, consequently, the high O_3 values decrease to oscillate around a relatively low value, where the tendency is to maintain those values, until a transition occurs again. The trends of Hurst exponents seem to correspond to the climatic conditions of Mexico City, where, in Spring, a climatic variable in this season is the high heat condition due to increased solar radiation. Which would imply higher levels of O_3 concentration at this time, by its very nature of formation and, which corresponds to the time where O_3 concentration rates are high, as observed by [11,35]. For the Summer and Autumn seasons in the same monitoring stations, H reveals

the three regimes with similar proportion of occurrence, summer 33.33%, which is antipersistent, followed by randomness with 30.56% and for persistence a rate of 36.11%. While for autumn there is an increase in the percentage of antipersistence with respect to summer of 36.11%, followed by a decrease with respect to the random regime with a percentage of 25%.

Finally, statistical persistence is characterized with a rate of 38.89%. In addition, Summer is an intermittence between hot days and rainy days, with greater and lesser solar radiation. This suggests high and low levels of O_3 concentration as reported by (Baldasano and Massagué 2017) where they found that pollutant records are lower during rainy times. In Autumn, the winds that help dissipate the O_3 predominate as reported by [52]. For Winter, the four monitoring stations show a well-defined Hurst exponent as antipersistent with an occurrence of 80.56%. This process indicates that the increments are independent and considered to be short memory processes.

The antipersistence in winter indicates that high or low O_3 concentration levels do not necessarily influence the values of subsequent records.

TABLE III. H obtained in period 2010-2018 for each monitoring station.

Season	Monitoring station	(H) Hurst exponent									Antipersistent	Randomness	Persistent
		2010	2011	2012	2013	2014	2015	2016	2017	2018			
	MER	0.524	0.504	0.614	0.608	0.515	0.472	0.622	0.607	0.467			
	XAL	0.434	0.668	0.620	0.627	0.428	0.424	0.575	0.533	0.588	$\overline{0.45}$	$\overline{0.50}$	$\overline{0.61}$
	TLA	0.536	0.493	0.580	0.594	0.463	0.462	0.639	0.550	0.445	19.44%	16.67%	63.89%
	CUA	0.621	0.480	0.697	0.682	0.567	0.536	0.668	0.671	0.553			
Summer	MER	0.512	0.636	0.478	0.520	0.528	0.449	0.419	0.487	0.311			
	XAL	0.568	0.636	0.444	0.576	0.552	0.475	0.344	0.465	0.292	$\overline{40}$	$\overline{0.50}$	$\overline{0.61}$
	TLA	0.487	0.637	0.414	0.585	0.536	0.452	0.519	0.491	0.438	33.33%	30.56%	36.11%
	CUA	0.560	0.666	0.516	0.636	0.626	0.562	0.371	0.471	0.391			
Autumn	MER	0.535	0.358	0.424	0.519	0.407	0.55	0.499	0.521	0.429			
	XAL	0.587	0.394	0.345	0.519	0.728	0.536	0.544	0.631	0.430	$\overline{0.39}$	$\overline{0.50}$	$\overline{0.60}$
	TLA	0.583	0.313	0.442	0.516	0.334	0.554	0.508	0.549	0.414	36.11%	25%	38.89%
	CUA	0.529	0.403	0.345	0.59	0.478	0.615	0.599	0.571	0.512			
Winter	MER	0.331	0.333	0.314	0.326	0.514	0.339	0.316	0.148	0.306			
	XAL	0.475	0.168	0.289	0.319	0.396	0.297	0.373	0.160	0.368	$\overline{0.32}$	$\overline{0.50}$	$\overline{0.58}$
	TLA	0.397	0.236	0.310	0.289	0.490	0.399	0.335	0.197	0.404	80.56%	16.67%	2.78%
	CUA	0.489	0.379	0.401	0.462	0.611	0.406	0.475	0.368	0.530			

In Winter, the decrease in solar radiation predominates, which would indicate lower concentration levels as reported by [7]. In addition, the O_3 concentration records in this season can be mostly attributed to those caused by vehicular traffic. That is indicated by the high proportion of toluene and xylenes, found in hydrocarbons, as the main source as referred by [12]. Although this is a case study, the results suggest that could be associate persistence with warm seasons, *i.e.* with higher solar incidence and higher incidence of records with high O_3 concentration indices. While antipersistence, could be associate it with cold seasons, *i.e.*, with lower solar incidence and lower incidence of high O_3 concentration records.

5. Conclusions

In this work it has been established that O_3 concentration levels are influenced by seasonal meteorological factors. The maximum values of O_3 concentration for a given hour of the day were observed during spring, while the minimum values were observed for winter. Between the two previous extremes were located the values for summer and autumn, which are very similar. This behavior is maintained throughout the study period, and it is independent of the monitoring site. Moreover, this behavior is congruent with the number of vehicle restriction measures taken by the city's environmental authorities, which occur mostly in spring, summer and autumn. Locally, the monitoring sites do show differences in the magnitudes of O_3 concentrations; however, since the highest values correspond both to the most industrialized areas and to the areas with the highest vehicular traffic, this behavior can be associated to the anthropogenic activities of

each monitoring site. It has been observed that the use of the fluctuation analysis and structure function technique are appropriate methods to characterize the power-law behavior (up to three orders of magnitude) of O_3 concentration levels for Mexico City. It was possible to characterize the power law trend of the O_3 fluctuation vs. time for each of the series of records for each season of the year by estimating the Hurst exponent. Using this method, it was possible to establish a correlation of persistence and antipersistence for spring and winter, respectively, in most cases. However, in some cases, the O_3 records show no correlation for the fluctuation function; that is, their processes are random. The Hurst exponent values for spring indicate statistical persistence and are therefore associated with long-range correlations. While those found for winter indicate statistical antipersistence, so they are associated with short-range correlations. On the other hand, the Hurst exponent values for summer and autumn were found to exhibit the three regimes of persistence, antipersistence and randomness, approximately in equal parts. Although this is a case study, the results suggest that could be associate persistence with warm seasons, *i.e.* with higher solar incidence and higher incidence of records with high O_3 concentration indices. While antipersistence, could be associate it with cold seasons, *i.e.*, with lower solar incidence and lower incidence of high O_3 concentration records. Finally, due to the large number of incidences, higher than the maximum allowed levels of O_3 concentration in spring and summer, it is recommended that for a better understanding of the temporal and spatial evolution of O_3 , a local analysis by zones and times of the year be considered; in addition to considering the influence of each of the anthropogenic variables specific to Mexico City.

1. K. Y. Kondratyev and C. A. Varotsos, Global total ozone dynamics, *Environmental Science and Pollution Research* **3** (1996) 153.
2. W. Lei, et al., Characterizing ozone production in the Mexico City Metropolitan Area: a case study using a chemical transport model, *Atmos. Chem. Phys.* **7** (2007) 1347.
3. J. Samet and D. Krewski, Health effects associated with exposure to ambient air pollution, *Journal of toxicology and environmental health, Part A* **70** (2007) 227.
4. L. Curtis *et al.*, Adverse health effects of outdoor air pollutants, *Environment international* **32** (2006) 815.
5. K. R. Smith, *Biofuels, air pollution, and health: a global review* (Springer Science & Business Media, 2013).
6. H. Zhao *et al.*, Investigation of ground-level ozone and high-pollution episodes in a megacity of Eastern China, *PloS one* **10** (2015) e0131878.
7. N. R. Awang *et al.*, Diurnal variations of ground-level ozone in three port cities in Malaysia, *Air Quality, Atmosphere & Health* **9** (2016) 25.
8. A. Gorai *et al.*, Influence of local meteorology and NO₂ conditions on ground-level ozone concentrations in the eastern part of Texas, USA, *Air Quality, Atmosphere & Health* **8** (2015) 81.
9. K. Binaku and M. Schmeling, Multivariate statistical analyses of air pollutants and meteorology in Chicago during summers 2010-2012, *Air Quality, Atmosphere & Health* **10** (2017) 1227.
10. S. Z. Azmi *et al.*, Trend and status of air quality at three different monitoring stations in the Klang Valley, Malaysia, *Air Quality, Atmosphere & Health* **3** (2010) 53.
11. N. R. Awang *et al.*, The influence of spatial variability of critical conversion point (CCP) in production of ground level ozone in the context of tropical climate, *Aerosol Air Qual Res.* **16** (2016) 153.
12. N. Bauri *et al.*, Evaluation of seasonal variations in abundance of BTXE hydrocarbons and their ozone forming potential in ambient urban atmosphere of Dehradun (India), *Air Quality, Atmosphere & Health* **9** (2016) 95.
13. J. M. Baldasano and J. Massagué, Trends and patterns of air quality in Santa Cruz de Tenerife (Canary Islands) in the period 2011-2015, *Air Quality, Atmosphere & Health* **10** (2017) 939.
14. D. Tarasick *et al.*, Quantifying stratosphere-troposphere transport of ozone using balloon-borne ozonesondes, radar wind-profilers and trajectory models, *Atmospheric Environment* **198** (2019) 496.
15. R. S. Williams *et al.*, Characterising the seasonal and geographical variability in tropospheric ozone, stratospheric influence and recent changes, *Atmos. Chem. Phys.* **19** (2019) 3589.
16. S. B. Shams *et al.*, Variations in the vertical profile of ozone at four high-latitude Arctic sites from 2005 to 2017, *Atmos. Chem. Phys.* **19** (2019) 9733.
17. T. Cieplak, T. Rymarczyk, and R. Tomaszewski, A concept of the air quality monitoring system in the city of Lublin with machine learning methods to detect data outliers (2019) <https://doi.org/10.1051/mateconf/201925203009>.
18. A. B. Chelani, Statistical persistence analysis of hourly ground level ozone concentrations in Delhi, *Atmospheric Research* **92** (2009) 244.
19. A. Gaur *et al.*, Four-year measurements of trace gases (SO₂, NO_x, CO, and O₃) at an urban location, Kanpur, in Northern India, *J. Atmospheric Chemistry* **71** (2014) 283.
20. M. Meraz *et al.*, Statistical persistence of air pollutants (O₃, SO₂, NO₂ and PM₁₀) in Mexico City, *Physica A: Statistical Mechanics and its Applications* **427** (2015) 202.
21. Z. Chen, C. P. Barros, and L. A. Gil-Alana, The persistence of air pollution in four mega-cities of China, *Habitat International* **56** (2016) 103.
22. L. Tohid *et al.*, Spatiotemporal variation, ozone formation potential and health risk assessment of ambient air VOCs in an industrialized city in Iran, *Atmospheric Pollution Research* **10** (2019) 556.
23. H. Guo *et al.*, Simulation of summer ozone and its sensitivity to emission changes in China, *Atmospheric Pollution Research* **10** (2019) 1543.
24. A. M. Diosdado, et al., Multifractal analysis of air pollutants time series, *Rev. Mex. Fis.* **59** (2013) 7.
25. C.-H. Shen, Y. Huang, and Y.-N. Yan, An analysis of multifractal characteristics of API time series in Nanjing, China, *Physica A: Statistical Mechanics and its Applications* **451** (2016) 171.
26. H.-d. He, Multifractal analysis of interactive patterns between meteorological factors and pollutants in urban and rural areas, *Atmospheric Environment* **149** (2017) 47.
27. Q. Dong, Y. Wang, and P. Li, Multifractal behavior of an air pollutant time series and the relevance to the predictability, *Environmental pollution* **222** (2017) 444.
28. Q. Wang, Multifractal characterization of air polluted time series in China, *Physica A: Statistical Mechanics and its Applications* **514** (2019) 167.
29. C. Xi *et al.*, A comparative study of two-dimensional multifractal detrended fluctuation analysis and two-dimensional multifractal detrended moving average algorithm to estimate the multifractal spectrum, *Physica A: Statistical Mechanics and its Applications* **454** (2016) 34.
30. H. L. Windsor and R. Toumi, Scaling and persistence of UK pollution, *Atmospheric Environment* **35** (2001) 4545.
31. C. A. Varotsos, J. M. Ondov, and M. Efstathiou, Scaling properties of air pollution in Athens, Greece and Baltimore, Maryland, *Atmospheric Environment* **39** (2005) 4041.
32. M. B. Musa and A. A. Jemain, Persistency of ozone concentrations in urban and suburban area of Peninsular Malaysia (2017). <https://doi.org/10.1063/1.4983870>.
33. A. Manju *et al.*, Spatio-seasonal variation in ambient air pollutants and influence of meteorological factors in Coimbatore, Southern India, *Air Quality, Atmosphere & Health* **11** (2018) 1179, <https://doi.org/10.1007/s11869-018-0617-x>.
34. M. L. Mansfield and C. F. Hall, Statistical analysis of winter ozone events, *Air Quality, Atmosphere & Health* **6** (2013) 687, <https://doi.org/10.1007/s11869-013-0204-0>.

35. A. Mukherjee, S. B. Agrawal, and M. Agrawal, Intra-urban variability of ozone in a tropical city-characterization of local and regional sources and major influencing factors, *Air Quality, Atmosphere & Health* **11** (2018) 965, <https://doi.org/10.1007/s11869-018-0600-6>.
36. A. S. Balankin, Dynamic scaling approach to study time series fluctuations, *Phys. Rev. E* **76** (2007) 056120.
37. Y.-H. Shao *et al.*, Comparing the performance of FA, DFA and DMA using different synthetic long-range correlated time series, *Scientific reports* **2** (2012) 835.
38. K. Hu *et al.*, Effect of trends on detrended fluctuation analysis, *Phys. Rev. E* **64** (2001) 011114.
39. U. Frisch, *Turbulence: The Legacy of A. N. Kolmogorov* (Cambridge University Press, 1996).
40. P. Meakin, The growth of rough surfaces and interfaces, *Physics Reports* **235** (1993) 189
41. A.-L. Barabási and T. Vicsek, Multifractality of self-affine fractals, *Physical Review A* **44** (1991) 2730.
42. M. Rak, *Fractals, Scaling and Growth Far from Equilibrium* (Universitetet i Oslo, 1999).
43. H.-O. Peitgen, H. J. $\frac{1}{4}$ rgens, and D. Saupe, *Chaos and fractals-new frontiers of science* (Springer-Verlag New York, 2004).
44. B. B. Mandelbrot and I. Stewart, Fractals and scaling in finance, *Nature* **391** (1998) 758.
45. WHO, Air quality guidelines for particulate matter, ozone, nitrogen dioxide and sulfur dioxide: global update 2005: summary of risk assessment (2006), <https://apps.who.int/iris/handle/10665/107823>.
46. SSA, Valor límite permisible para la concentración de ozono (O_3) en el aire ambiente y criterios para su evaluación (2014), https://www.dof.gob.mx/nota_detalle.php?codigo=5356801&fecha=19/08/2014.
47. I. Jhun *et al.*, The impact of nitrogen oxides concentration decreases on ozone trends in the USA, *Air Quality, Atmosphere & Health* **8** (2015) 283.
48. A. Monteiro *et al.*, Investigating ozone episodes in Portugal: a wavelet-based approach, *Air Qual Atmos Health* **9** (2016) 775.
49. A. Sharma *et al.*, Influence of ozone precursors and particulate matter on the variation of surface ozone at an urban site of Delhi, India, *Sustainable Environment Research* **26** (2016) 76.
50. A. Kumar *et al.*, Dynamic interaction of trace gases (VOCs, ozone, and NOx) in the rural atmosphere of sub-tropical India, *Air Quality, Atmosphere & Health* **10** (2017) 885.
51. M. A. Iqbal *et al.*, Comparison of ozone pollution levels at various sites in Seoul, a megacity in Northeast Asia, *Atmospheric Research* **138** (2014) 330.
52. E. Kovač-Andrić, J. Brana, and V. Gvozdić, Impact of meteorological factors on ozone concentrations modelled by time series analysis and multivariate statistical methods, *Ecological Informatics* **4** (2009) 117, <https://doi.org/10.1016/j.ecoinf.2009.01.002>.
53. C.-Z. Yao, J.-N. Lin, and X.-Z. Zheng, Coupling detrended fluctuation analysis for multiple warehouse-out behavioral sequences, *Physica A: Statistical Mechanics and its Applications* **465** (2017) 75.